AIP | Journal of Applied Physics

Acoustic confinement and waveguiding with a line-defect structure in phononic crystal slabs

Abdelkrim Khelif, Saeed Mohammadi, Ali Asghar Eftekhar, Ali Adibi, and Boujamaa Aoubiza

Citation: J. Appl. Phys. 108, 084515 (2010); doi: 10.1063/1.3500226
View online: http://dx.doi.org/10.1063/1.3500226
View Table of Contents: http://jap.aip.org/resource/1/JAPIAU/v108/i8
Published by the American Institute of Physics.

Acoustic confinement and waveguiding with a line-defect structure in phononic crystal slabs

Abdelkrim Khelif,[1,a)] Saeed Mohammadi,[2] Ali Asghar Eftekhar,[2] Ali Adibi,[2] and Boujamaa Aoubiza[3]

[1]*International Joint Laboratory, Georgia Tech-CNRS UMI 2958, 2-3 Rue Marconi, 57070 Metz, France and Institut FEMTO-ST, CNRS, Université de Franche-Comté, 32 avenue de l'Observatoire 25044 Besançon Cedex, France*

[2]*School of Electrical and Computer Engineering, Georgia Institute of Technology, Atlanta, Georgia 30332, USA*

[3]*Laboratoire de Mathématiques, Université de Franche-Comté, route de Gray, 25030 Besançon Cedex, France*

(Received 1 July 2010; accepted 14 August 2010; published online 28 October 2010)

We present a new way of forming phononic crystal waveguides by coupling a series of line-defect resonators. The dispersion proprieties of these coupled resonator acoustic waveguides (CRAW) can be engineered by using their geometrical parameters. We show that single-mode guiding over a large bandwidth is possible in CRAW formed in a honeycomb-lattice phononic crystal slab of holes in zinc oxide. In addition, a finite length of CRAW structure acts as an efficient selective acoustic filter for Lamb waves. © *2010 American Institute of Physics*. [doi:10.1063/1.3500226]

I. INTRODUCTION

In the last two decades, a great effort has been devoted to the study of the so-called phononic crystals.[1–5] These structures, constituted of a periodic repetition of inclusions in a matrix background, are for acoustic or elastic waves in solids and in fluids the analogs of photonic crystals for optical or electromagnetic waves.[6,7] Several classes of phononic crystals have received attention, which differ mainly by the physical and geometrical nature of the inclusions and by the matrix. We can find among them the solid/solid, fluid/fluid, and mixed solid/fluid composite systems. They typically exhibit stop bands in their transmission spectra for which the propagation of sound or vibration can be strictly forbidden in all directions of propagation. In other words, they play the role of perfect mirrors for elastic or acoustic waves in the frequency range of the band gap. The location and width of the obtained band gaps result from the choice of the lattice, the shape of the inclusions, and the constitutive materials.

The fundamental interest in controlling the elastic energy and the subsequent foreseeable applications of phononic crystals are now well established. An ingenious use of the concept of band gap can allow the propagation of elastic or acoustic waves to be regulated. They can indeed be used to filter, confine, or guide acoustic energy, which may lead to new prospects in a variety of applications including wireless communications and sensing.

Various types of acoustic and elastic wave propagation have been studied in different classes of phononic structures. The studies of the propagation of bulk waves in two- or three-dimensional phononic crystals include the analysis of the band gap effect in finite structures as well as the confinement and guiding of acoustic energy through the use of defect inclusions in the perfect phononic crystal structures.[8,9] The surface wave in semi-infinite phononic crystals with cylindrical holes etched in a single material or a solid/solid composition have already been studied.[10–14] Recently, the guided waves in phononic crystal slabs have attracted more attention due to the natural confinement of elastic energy within the slab. Different configurations of phononic crystal slabs including the cylindrical holes etched in unsupported membrane[15,16] and solid/solid compositions with the cylindrical rods inserted[17–19] or deposited on the top of the slab[20,21] have been proposed to provide omnidirectional phononic band gaps. The formation of functional devices like waveguides and resonators by adding defects to a perfect phononic crystal have been reported.[16,19] Typically waveguide is formed by adding a line defect (e-g., by removing one row of holes) to a perfect crystal. Resonator can be formed by adding either a point defect or a line defect in the form of a Fabry–Perot structure.[22]

In this paper, we present a new form of waveguiding in phononic crystals formed by coupling a series of the line-defect resonators. These structures, which we refer to as coupled resonator acoustic waveguides (CRAW), provide us the flexibility of engineering their dispersion using only geometrical parameters. In addition, by selecting a finite length of CRAW, filtering of acoustic signals can be achieved. In Sec. II, we discuss the details of the model and the method of calculation. The results for the CRAW are presented in Sec. III and the conclusion of the paper in Sec. IV.

II. MODEL AND METHOD OF CALCULATION

We consider a honeycomb-lattice array of cylindrical hole etched in a free standing membrane as illustrated in Fig. 1. The z axis is chosen to be perpendicular to the surface. The lattice parameter of the phononic crystal is a. The filling fraction is defined as $F=(4/3)\sqrt{3}\pi r^2/a^2$, where r is the radius of the holes. The thickness of the membrane is h. Dispersion curves are calculated for the prefect phononic crystal using a finite element method, where only the unit cell is

a)Electronic mail: abdelkrim.khelif@gatech.edu.

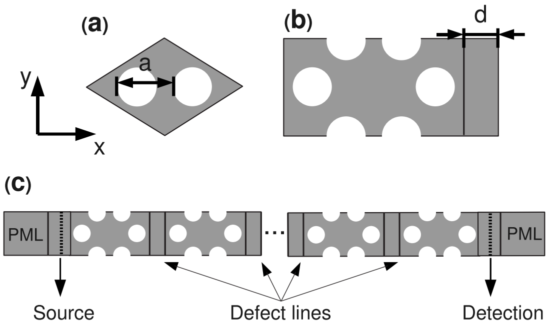

FIG. 1. In plane projection of the phononic crystal slab composed of a honeycomb-lattice array of cylindrical holes etched in free standing membrane. The lattice parameter is a and the holes have radius r. The thickness of slab is h. (a) The unit cell domain used for band diagram calculations is meshed in three dimensions and Bloch–Floquet periodic boundary conditions are applied. (b) Super cell unit for band diagram calculations for a coupled resonator structure. (c) The domain used for transmission computations has periodic boundary conditions along the y direction and a finite extent along the x direction. PMLs are used to prevent reflections from the domain boundaries. A line source generates waves propagating in the x direction. The transmitted signals are collected in the detection line.

meshed, and Bloch–Floquet conditions are implemented via periodic boundary conditions.[17] In the case of the perfect structure without defect as depicted in Fig. 1(a), a three-dimensional mesh is used, and the structure is assumed to be infinite and periodic in both the x and y directions. A phase relation is applied on the lateral sides of the unit cells, defining boundary conditions between adjacent cells. This phase relation is related to the Bloch wave number of the modes of the periodic structure. By varying the wave vector in the first Brillouin zone and solving an eigenvalue problem, the eigenfrequencies are obtained. The eigenvectors in this case, represent the modal displacement fields. To introduce the defect like coupled resonators of Fig. 1(c), we use the supercell technique, where phase change is enforced only in one direction, i.e., x, and the structure is repeated in the y direction with zero phase shift. The computation domain in this case is shown in Fig. 1(b).

For transmission calculations, the model depicted in Fig. 1(c) is used. An acoustic wave with a specific polarization (u_x, u_z, u_y) is modeled by applying a line source vibrating on the surface. We apply a periodic boundary condition in the y direction, which emulates an infinitely long line source. This line source, will generate propagating waves in the (x direction with uniform phase fronts along the y direction. To prevent reflections caused by wave scattering from the domain boundaries, perfectly matched layers (PMLs) (Ref. 23) are applied as illustrated in Fig. 1(c). PMLs have the property of gradually absorbing mechanical disturbances in a given layer without causing a reflection.[24] Consequently, PMLs will not disturb the propagation of the acoustic waves, emulating infinite media. We can write the governing equation of a PML as

$$\frac{1}{\gamma_j(\mathbf{r})}\frac{\partial T_{ij}}{\partial x_j} = -\rho\omega^2 u_i, \tag{1}$$

where ρ is the mass density of the material, and ω is the angular frequency. Summation over repeated indices is implicitly assumed. T_{ij}; are the stress tensors, u_i; are the displacement components and the x_j are the coordinates $(x_1 = x,\ x_2 = y,\ x_3 = z)$. The function $\gamma_j(\mathbf{r})$ is the artificial damping along the x_j axis at an arbitrary position $\mathbf{r}$ inside the PML. As PMLs are added to attenuate acoustic waves propagating in the x direction, only γ_x is different from 1, and is given by

$$\gamma_x(x) = 1 - i\sigma_x(x - x_l)^2, \tag{2}$$

where x_l is the coordinate of the interface between the regular domain and the PML and σ_x is a constant. There is no damping outside the PMLs and here $\gamma_j = 1$ is assumed. A suitable thickness for the PML as well as for the value of σ_x must then be found by trial calculations so that mechanical disturbances are absorbed before reaching the outer boundaries. The absorption must also be sufficiently gradual so that reflections occurring at the interface between the regular domain and the PML are kept minimal.[23] The mechanical stresses T_{ij} further depend on the strains as

$$T_{ij} = C_{ijkl}S_{kl}, \tag{3}$$

where the C_{ijkl} are the elastic stiffness constants. Strains are related to the displacements following:

$$S_{ij} = \frac{1}{2}\left(\frac{1}{\gamma_j}\frac{\partial u_i}{\partial x_j} + \frac{1}{\gamma_i}\frac{\partial u_j}{\partial x_i}\right). \tag{4}$$

III. RESULTS AND DISCUSSION

It is well known that a complete and large band gap is needed to confine the elastic energy by introducing a defect in a phononic crystal structure. Recently, we have studied different geometrical parameters and lattice symmetries of a two-dimensional array of etched holes in free standing silicon membranes.[15] We showed a large band gap with a relatively low filling fraction occurs in a honeycomb-lattice array of holes. In this case, the two parameters that can play an important role in the chosen geometry are the thickness of the slab and the radius of the holes. We calculated the band diagrams of the phononic crystal slab depicted in Fig. 1(a) for a phononic crystal formed in a zinc oxide slab. Propagation, here, is in the (x, y) plane, and the band diagrams are generated along the high symmetry axes of the first Brillouin zone. Figure 2 shows the structure has an absolute band gap in the band structure with a relative radius $(r/a = 0.43)$ and relative slab thickness $(h/a = 1)$. The band gap extends from 850 to 1150 m/s, and holds for all polarizations and directions of propagation in the slab. Indeed, the phononic crystal slabs surrounded by vacuum, naturally provide a perfect confinement of waves in the vertical direction, and the added two-dimensional structure produces an in-plane band gap.

It is well established that the addition of defects to a perfect phononic crystal with a complete phononic band gap allows for the design of devices like waveguides and cavities to control the propagation of acoustic waves inside the band gap and to enable novel functionalities in a very compact structure. Usually, the defects are created by removing or modifying a number of inclusions. In this work, we have selected to add a line defect of solid material with "d" width between two holes in ΓK direction of reduced Brillouin

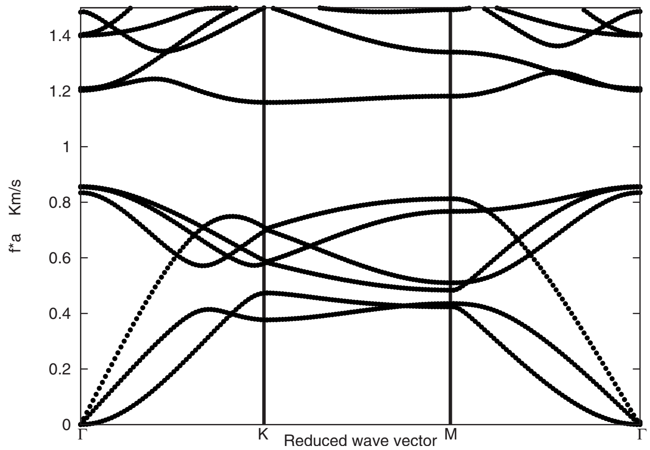

FIG. 2. Band diagram of a honeycomb-lattice phononic crystal slab composed of cylindrical holes etched in a zinc oxide slab, calculated along high symmetry directions of the first irreducible Brillouin zone. The lattice parameter is a and the relative radius $r/a=0.43$. The relative thickness of the slab h/a is equal to 1.

zone. In this defect structure, we conserve the translational symmetry along the x direction as pictured in Fig. 1(b). Basically, the line defect acts as a single resonator and the coupling between those single resonators is managed by the number of periods that separate two successive line defects. First, we simulated the band diagram of line defect of width $d/a=1$ and, the successive line defects are separate by two periods of the lattice in the propagating direction. We used a supercell technique, where the phase change is injected only in one direction (i.e., x). The structure is repeated in the orthogonal direction (i.e., y) with a zero phase change. The band diagram is illustrated in Fig. 3, which exhibits three flat bands within the central band gap region related to the presence of the line defect. The flatness of the bands indicates that the group and energy velocities are approximately equal to zero, and the displacements are spatially confined. This signature supposes that two periods separation ensures the elimination of the overlapping between the displacement fields of the two line defects and each line defect is therefore, isolated from other defects. In order to corroborate these observations, we plot in Figs. 4 the out-of-plane displacement field of the first band in Fig. 3 ($f\times a=0.975$ km/s). The wave vector k_x selected for this illustration is close to the limit of the first Brillouin zone. We emphasize that the acoustic energy is mostly confined to the line defect, and the structure acts as an acoustic single resonator.

As shown in the Fig. 4, the two-period distance between the defects provides a good isolation of the resonators, and the acoustic energy, therefore, will be confined to the line defect. However, to allow the propagation of the acoustic energy and achieve waveguiding functionality, an efficient acoustic coupling between the resonators is needed. To obtain such efficient coupling, the separation between two successive resonators is reduced to one period. The band diagram of such structure is shown in Fig. 5. Adjacent defects affect the flatness of the bands resulting in a nonzero group velocity, which leads to the transfer of the acoustic energy through these coupled defects. This designed waveguide has the advantage to control the dispersion and the group velocity through the geometrical parameters. In Fig. 5, where two values of the relative width of the line defect (i.e., $d/a=1.10$ and $d/a=1.15$) are plotted, we can distinguish a range of frequency with single-mode characteristics for these

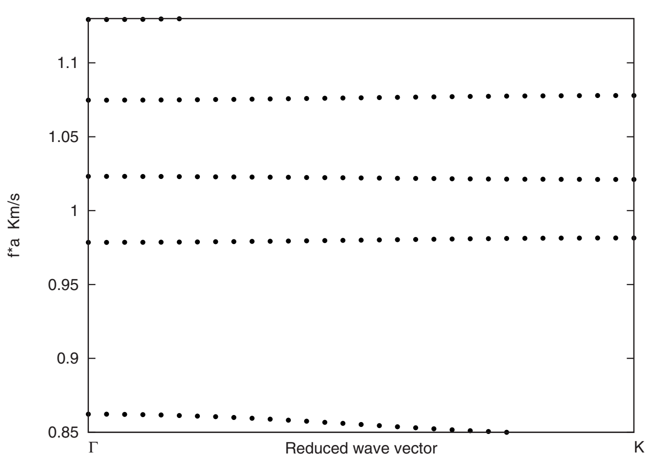

FIG. 3. Band diagram of a line-defect waveguide made using a phononic crystal slab. The associated supercell is composed of two complete periods of the phononic crystal structure separating the line defect. the propagation is considered to be along ΓK direction in the reciprocal lattice. The relative width of line defect is equal to $d/a=1$.

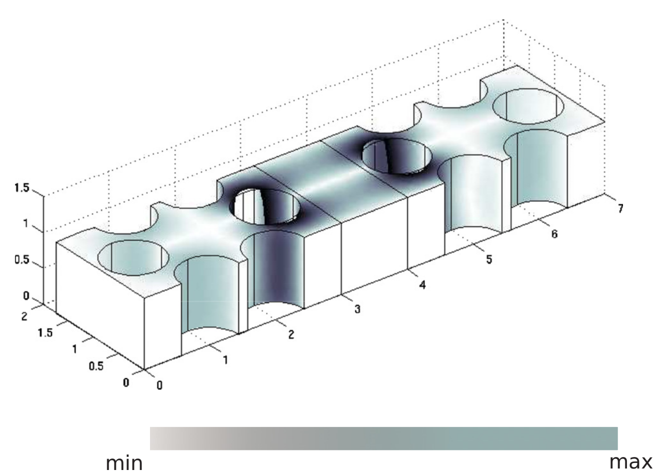

FIG. 4. (Color online) Out of plane displacement filed distribution of first band ($f\times a=0.975$ km/s) in Fig. 3. The wave vector k_x selected is close to the limit of the first Brillouin zone.

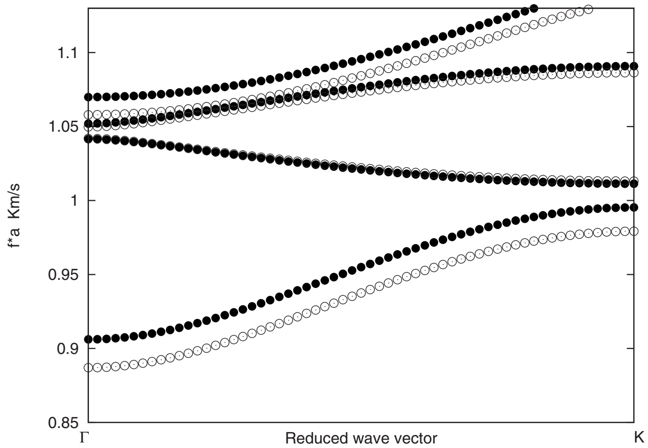

FIG. 5. Band diagram of a coupled resonator waveguide made using a phononic crystal slab composed of cylindrical holes etched in a zinc oxide slab. The supercell unit is composed by one period separation from the adjacent line defect. The propagation is considered along ΓK direction. The relative width of line-defect is equal to $d/a=1.10$ (filled dot) and $d/a=1.15$ (hollow dot).

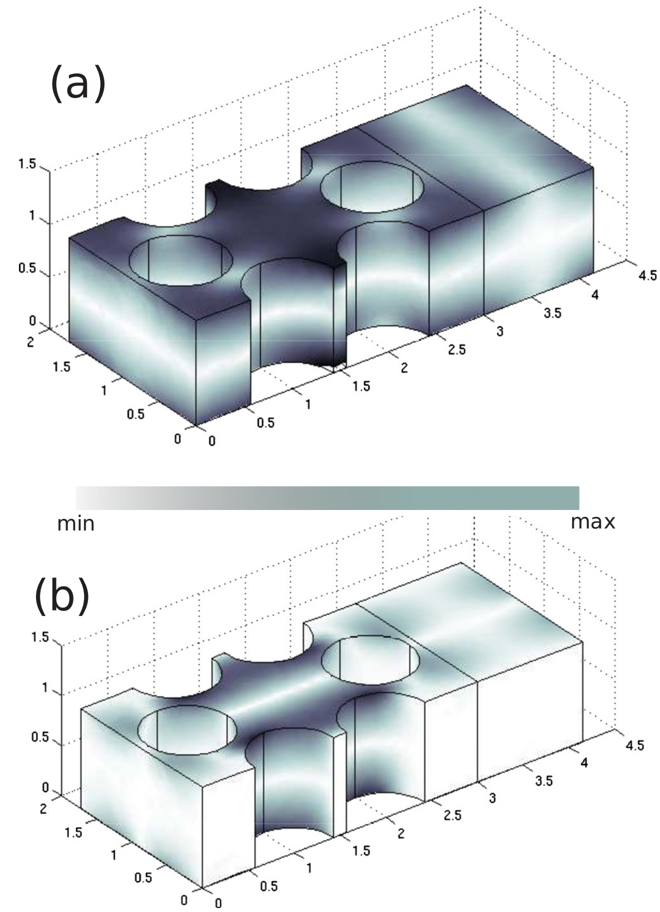

FIG. 6. (Color online) Distribution of the out of plane displacement field for the coupled resonator waveguide analyzed in Fig. 5. The wave vector value is close to the limit of the Brillouin zone for band 1 (a) and 2 (b).

waveguides. This single mode occurs within the omnidirectional bang gap of the phononic crystal slab in the frequency range $(0.87 < f\times a < 1.0)$ for the first band in Fig. 5. Besides the separation between the line defect, the relative width d/a can play a role in the dispersion of the waveguide. Indeed, when the line-defect width is increased from $d/a=1.10$ to $d/a=1.15$, we can notice that the sensitivity of the waveguide modes to the relative width is not equivalent for all the bands. Especially, the second and the third bands remain at the same position for both line-defect width values, while the first and fourth bands are shifted down toward lower frequencies. To understand this behavior, we calculated the mode profiles for bands 1 and 2 in Fig. 6 for the waveguide with $d/a=1.10$. We observe that for the first band, the displacement field is distributed within the line defect in the unit cell, while it is mostly localized outside of the defect for the second band. This can explain the sensitivity and insensitivity of the first and second bands to the line-defect width, respectively.

The results described so far are obtained for the structures with infinite periodicity. To evaluate the effect of the finite size, which is very important for practical realization, the transmission spectra were computed for elastic waves propagating along the x direction using the domain depicted in Fig. 1(c). The domain is finite along x with five resonators sandwiched between the input and the output media. As discussed in Sec. II, the structure is infinite and periodic along y direction. A line source is placed on the surface of the slab on one side of the phononic crystal structure. This line source vibrates at a monochromatic frequency and can have two different polarizations: (i) (u_x,u_z), sagittal displacements that can excite the lamb waves of the homogeneous slab, and (ii) u_y, transverse displacements that can be considered as a shear horizontal wave source of excitation.

Figure 7 displays the computed transmission spectra for the sagittal and the shear horizontal polarization line sources. Transmissions are computed for the ΓK direction of the band diagrams. The band diagram is also added to Fig. 7 to help with the interpretation of the results. In Fig. 7(a), the band diagram shows four branches of the waveguide starting at $f\times a=0.89$ km/s. The transmission in Fig. 7(b) shows the total displacement (i.e., $|u_x|+|u_z|+|u_y|$) collected in the detection line of a sagittal source (u_x,u_z) (straight line) and shear source (u_y) (dashed line) excitations. In the case of sagittal source, one pass band is apparent corresponding to the first branch in the band diagram. The CRAW structure acts, here, as an acoustic filter where the relative bandwidth of the filter can be managed by the interaction between the resonators. We notice several oscillations appear in this pass band of the filter which indicate the back-and-forth travel of the wave inside the five coupled resonator structure due to the acoustic impedances mismatch between the CRAW structure and the homogeneous slab. The higher bands do not have significant transmission to the sagittal excitation and act as deaf band. Besides, in the case of shear source excitation, we note a very low magnitude in the transmission for the first band, and a significant transmission for the higher bands. Obviously, the use of the CRAW structure as an acoustic filter is more suitable for sagittal waves (Lamb waves) than the shear one where the transmission spectra are more complex. Besides, the relative bandwidth of the filter is 10% which can be very useful for practical realization of acoustic filtering devices.

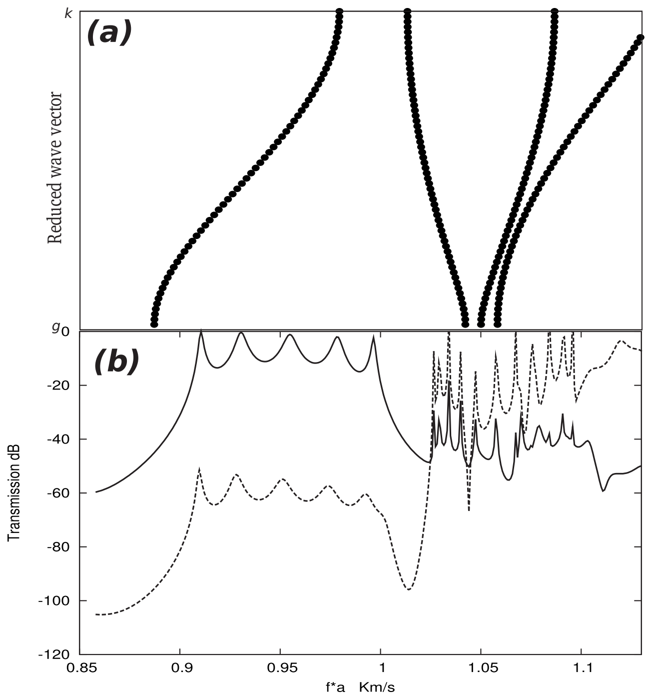

FIG. 7. Transmission of guide waves through five resonators in the phononic crystal slab. (a) Band diagram for guided waves propagating along the ΓK direction. (b) Computed transmission spectrum with a sagittally polarized excitation line source (straight line) and shear horizontally polarized excitation line source (dashed line). Transmissions represent an average of all displacement components, $|u_x|+|u_z|+|u_y|$, as a function of frequency. The average is collected along a line located after the fifth period.

IV. CONCLUSION

In this paper, we have studied the possibility of forming a new phononic crystal waveguide that can be used as an acoustic filter device. The filter is based on the confinement and guiding of the acoustic energy in a phononic crystal slab. The structures are made by etching a honeycomb array of holes in a free standing slab. This phononic slab structure exhibits an absolute phononic band gap for all polarizations of the guided waves inside the slab. A line defect is introduced which allow to confine spatially the acoustic energy and to achieve an acoustic resonator. Besides, we presented a waveguide in phononic crystal slabs composed of several single resonators that are coupled periodically through evanescent waves. We illustrated the considerations that must be applied to achieve single-mode guided bands in these systems. The waveguide acted as selective acoustic filter, where the acoustic energy is localized in the extended defect formed by the collective behavior of the coupled resonators. The frequencies of the filters are sensitive to the geometrical parameters of the defect line and to the separation distance between the single resonators. The transmission through the finite size structure shows the importance of the polarization of the propagation wave. The numerical simulations are performed using the finite element method and considering a zinc oxide slab.

[1]M. M. Sigalas and E. N. Economou, Solid State Commun. **86**, 141 (1993).
[2]M. S. Kushwaha, P. Halevi, L. Dobrzynski, and B. Djafari-Rouhani, Phys. Rev. Lett. **71**, 2022 (1993).
[3]T. Miyashita, Meas. Sci. Technol. **16**, R47 (2005).
[4]An exhaustive list of references on phononic crystals can be found at http://www.phys.uoa.gr/phononics/PhononicDatabase.html
[5]I. E. Psarobas, Z. Kristallogr. **220**, IV (2005).
[6]E. Yablonovitch, Phys. Rev. Lett. **58**, 2059 (1987).
[7]S. John, Phys. Rev. Lett. **58**, 2486 (1987).
[8]J. O. Vasseur, P. A. Deymier, B. Chenni, B. Djafari-Rouhani, L. Dobrzynski, and D. Prevost, Phys. Rev. Lett. **86**, 3012 (2001).
[9]A. Khelif, B. Djafari-Rouhani, J.-O. Vasseur, and P. A. Deymier, Phys. Rev. B **68**, 024302 (2003).
[10]Y. Tanaka and S. Tamura, Phys. Rev. B **58**, 7958 (1998).
[11]T.-T. Wu, Z.-G. Huang, and S. Lin, Phys. Rev. B **69**, 094301 (2004).
[12]T.-T. Wu, L.-C. Wu, and Z.-G. Huang, J. Appl. Phys. **97**, 094916 (2005).
[13]V. Laude, M. Wilm, S. Benchabane, and A. Khelif, Phys. Rev. E **71**, 036607 (2005).
[14]S. Benchabane, L. Robert, J.-Y. Rauch, A. Khelif, and V. Laude, Phys. Rev. E **73**, 065601 (2006).
[15]S. Mohammadi, A. Eftekhar, A. Khelif, H. Moubchir, R. Westafer, W. Hunt, and A. Adibi, Electron. Lett. **43**, 898 (2007).
[16]S. Mohammadi, A. Eftekhar, A. Khelif, W. Hunt, and A. Adibi, Appl. Phys. Lett. **92**, 221905 (2008).
[17]A. Khelif, B. Aoubiza, S. Mohammadi, A. Adibi, and V. Laude, Phys. Rev. E **74**, 046610 (2006).
[18]F.-L. Hsiao, A. Khelif, H. Moubchir, A. Choujaa, C.-C. Chen, and V. Laude, Phys. Rev. E **76**, 056601 (2007).
[19]I. El-Kady, R. H. Olsson, and J. G. Fleming, Appl. Phys. Lett. **92**, 233504 (2008).
[20]T.-C. Wu, T.-T. Wu, and J.-C. Hsu, Phys. Rev. B **79**, 104306 (2009).
[21]Y. Pennec, B. Djafari-Rouhani, H. Larabi, J. O. Vasseur, and A. C. Hladky-Hennion, Phys. Rev. B **78**, 104105 (2008).
[22]S. Mohammadi, A. Eftekhar, W. Hunt, and A. Adibi, Appl. Phys. Lett. **94**, 051906 (2009).
[23]J.-P. Berenger, J. Comput. Phys. **114**, 185 (1994).
[24]M. B. Dühring, V. Laude, and A. Khelif, J. Appl. Phys. **105**, 093504 (2009).